Mol. Cells *33*, 553-562, June 30, 2012
DOI/10.1007/s10059-012-2269-2

Molecules and Cells

Lentiviral Vector-Mediated shRNA against AIMP2-DX2 Suppresses Lung Cancer Cell Growth through Blocking Glucose Uptake

Seung-Hee Chang[1,9], Youn-Sun Chung[1,9], Soon-Kyung Hwang[2], Jung-Taek Kwon[1,3], Arash Minai-Tehrani[1], Sunghoon Kim[4], Seung Bum Park[5], Yeon-Soo Kim[6], and Myung-Haing Cho[1,7,8,*]

Aminoacyl-tRNA synthetases [ARS]-interacting multifunctional protein 2 (AIMP2) has been implicated in the control of cell fate and lung cell differentiation. A variant of AIMP2 lacking exon 2 (AIMP2-DX2) is expressed in different cancer cells. We previously studied the expression level of AIMP2-DX2 in several lung cell lines and reported elevated expression levels of AIMP2-DX2 in NCI-H460 and NCI-H520. Here, we report that the suppression of AIMP2-DX2 by lentivirus mediated short hairpin (sh)RNA (sh-DX2) decreased the rate of glucose uptake and glucose transporters (Gluts) in NCI-H460 cells. Down-regulation of AIMP2-DX2 reduced glycosyltransferase (GnT)-V in the Golgi apparatus, while inducing the GnT-V antagonist GnT-III. Down-regulation of AIMP2-DX2 also suppressed the epidermal growth factor receptor/mitogen activated protein kinase (EGFR/MAPK) signaling pathway, leading to the decrease of the proliferation marker Ki-67 expression in nuclei. Furthermore, dual luciferase activity reduced cap-dependent protein translation in cells infected with sh-DX2. These results suggest that AIMP2-DX2 may be a relevant therapeutic target for lung cancer, and that the sh-DX2 lentiviral system can be an appropriate method for lung cancer therapy.

INTRODUCTION

Aminoacyl-tRNA synthetases (ARSs) are essential enzymes that join amino acids to transfer RNAs, linking the genetic code to specific amino acids. ARSs participate in a wide variety of functions, including transcription, translation, splicing, inflammation, angiogenesis and apoptosis. Three nonenzymatic proteins, ARS-interacting multifunctional proteins (AIMPs), associate with ARSs in a multi-synthetase complex of higher eukaryotes (Park et al., 2005). AIMP2 (previously known as both p38 and JTV-1) is associated with a multi-ARS complex and interacts with AIMP1 *via* its coiled-coil leucine zipper motif. It is regulated for lung cell differentiation (Kim et al., 2003) and is also implicated in the control of neural cell death (Ko et al., 2005). Upon transforming growth factor-beta (TGF-β) treatment, AIMP2 is translocated to the nucleus and binds to the far upstream element (FUSE)-binding protein (FBP) (Kim et al., 2003), which is a transcriptional activator of *c-myc* gene (Duncan et al., 1994). AIMP2 binding stimulates ubiquitination and proteasomal-dependent degradation of FBP. These events lead to down-regulation of c-myc, which is required for differentiation of functional alveolar type II cells (Kim et al., 2003). AIMP2-DX2 is named for the variant of AIMP2 that has a deletion in exon 2, and which is specifically expressed in a variety of cancer cells including lung cancer, breast cancer, liver cancer, stomach cancer and bone cancer (Kim, 2004; 2005). Therefore, the use of specific short hairpin (sh)RNA to suppress the expression of AIMP2-DX2 may be a rational therapeutic strategy for treatment of cancer.

Glucose is the most important energy source for cell growth. Fast-growing cancer cells require more glucose than normal cells do. Glucose passage across cell membranes is mediated by a family of transporters termed glucose transporter (Glut). Glucose uptake in non-small cell lung cancer (NSCLC) is related to Glut-1, which is a significant indicator of poor prognosis in NSCLC (Younes et al., 1997). Protein glycosylation has an important role in many cellular processes, including cell growth, cell-cell interactions, cancer metastasis, differentiation and development. Using a systems-level approach to investigate the concentration between glycosylation and cellular function, Lau et al. (2007) demonstrated a fine-tuning mechanism for switching from growth to arrest in cells based on the flux of UDP-GlcNAc through the Golgi and the extent of N-glycan

[1]Laboratory of Toxicology, College of Veterinary Medicine, Seoul National University, Seoul 151-742, Korea, [2]Gene Regulation Section, Laboratory of Cancer Prevention, Center for Cancer Research, National Cancer Institute, Frederick, MD 21702, USA, [3]Risk Assessment Division, National Institute of Environmental Research, Incheon 404-708, Korea, [4]Medicinal Bioconvergence Research Center, Seoul National University, Seoul 151-742, Korea, [5]Department of Chemistry, College of National Science, Seoul National University, Seoul 151-742, Korea, [6]Department of Smart Foods and Drugs and Indang Institute of Molecular Biology, Inje University, Seoul 100-032, Korea, [7]Department of Nanofusion Technology, Graduate School of Convergence Science and Technology, Seoul National University, Seoul 151-742, Korea, [8]Graduate Group of Tumor Biology, Seoul National University, Seoul 151-742, Korea, [9]These authors contributed equally to this work.
*Correspondence: mchotox@snu.ac.kr

Received November 25, 2011; revised March 20, 2012; accepted March 22, 2012; published online May 4, 2012

Keywords: AIMP2-DX2, EGFR/MAPK signaling pathway, glucose uptake, gluts

branching of growth factor receptors.

Here, we report that the down-regulation of AIMP2-DX2 expression by lentiviral-based shRNA can suppress glucose uptake and decrease cancer cell growth through the alteration of the epidermal growth factor receptor/mitogen activated protein kinase (EGFR/MAPK) signaling pathway. These results suggest that AIMP2-DX2 may be a relevant therapeutic target for lung cancer, and that lentiviral vector-based shRNA method targeting of AIMP2-DX2 can be an appropriate method for treatment of lung cancer.

MATERIALS AND METHODS

Reagents, plasmid and antibodies

Penicillin-streptomycin was purchased from GibcoBRL (USA). Freund's complete adjuvant, Freund's incomplete adjuvant, anti-mouse IgG-fluorescein isothiocynate (FITC), anti-rabbit IgG FITC conjugate, anti-Goat IgG FITC conjugate, 4′, 6-diamidino-2-phenylindole (DAPI), 6-diazo-5-oxo-L-norleucine (DON) and cytochalasin B were purchased from Sigma-Aldrich (USA). Anti-Glut-1, anti-Glut-2, anti-Glut-3, anti-Glut-4, anti-GnT-III, anti-GnT-V, anti-phospho-EGFR (Tyr1173), anti-K-ras, anti-ERK1/2, anti-Mnk1, anti-eIF4E and anti-Ki-67 antibodies were obtained from Santa Cruz Biotechnology (USA). Anti-O-linked N-acetylglucosamine was purchased from Affinity BioReagents (USA). Anti-EGFR was purchased from Cell Signaling Technology (USA). Anti-glyceraldehyde 3-phosphate dehydrogenase (GAPDH) was purchased from AbFrontier (Korea). Monoclonal AIMP2-DX2 antibody was prepared as described previously (Kim, 2004; 2005). The bicistronic construct, pcDNA-fLUC-polIRES-rLUC, was a kind gift from Dr. Gram (Novartis Pharma AG, Switzerland).

Production of lentivirus for siRNA targeting of AIMP2-DX2

Five small interfering (si)RNA sequences targeting human AIMP2-DX2 mRNA were designed. The best sequences for down-regulating AIMP2-DX2 expression were si-AIMP2-DX2 #4 (5′-GCUGGCCACGUGCAGGAUUAC-3′) and si-AIMP2-DX2 #5 (5′-CACGUGCAGGAUUACGGGGC-3′) (Kim, 2004; 2005). Scrambled sequence (5′-AAUCGCAUAGCGUAUGC CGUU-3′) was used as a control. shRNA was generated based on above siRNA sequences and cloned into pENTR/U6™ entry vector (Invitrogen, USA). The cassettes containing U6 promoter and shRNA-target sequences were transferred to a lentivirus vector (pLenti6/BLOCK-iT™-DEST vector) following the manufacturer's instructions (BLOCK-iT™ Lentiviral RNAi Expression System; Invitrogen). Recombinant lentiviral vectors were packaged using ViraPower™ Lentiviral Packaging Mix (Invitrogen) and the virus titer was determined using HIV 1 p24 ELISA KIT (PerkinElmer Life Sciences, USA). Lentiviral vector-medited shRNA targeting AIMP2-DX2 #4 and AIMP2-DX2 #5 were referred to sh-DX2 #4 and sh-DX2, respectively. Lentiviral delivery of shRNA of non-specific targeting (scramble) was referred to sh-scr.

Cell culture and lentivirus infection

WI-38 (normal control), A549, NCI-H226, -H322, -H460, and -H520 NSCLC cells were cultured in RPMI 1640 supplemented with 10% fetal bovine serum (FBS), 100 units/ml penicillin G sodium and 100 μg/ml streptomycin sulfate in a humidified incubator in an atmosphere of 5% CO_2 at 37°C. NCI-H460 (American Type Culture Collection number HTB-177) cells were seeded in a T25 or T75 flask 24 h before lentivirus infection, then infected with lentivirus containing shRNA targeting AIMP2-DX2 and scramble (p24, 10 ng/ml) for 24 h. The medium was were removed and replaced with fresh medium. After additional incubation for 48 h, cells were harvested for future experiments.

RT-PCR

Total RNA was isolated using TRIzol Reagent (Invitrogen), and subjected to RT-PCR ONE-STEP RT-PCR PreMix Kit (iNtRON Biotechnology, Korea) following the manufacturer's protocol. Two micrograms RNA were amplified with specific primers at the following cycling conditions: RT step - reverse transcription reaction at 45°C for 30 min, denaturation of RNA: cDNA hybrid at 94°C for 5 min; PCR step - denaturing at 94°C for 60 s, annealing at 53°C for 60 s, and extension at 72°C for 60 s, 35 cycles. GAPDH was amplified as an internal standard. The sequences of primers used for RT-PCR were: AIMP2-DX2, forward (5′-ATGCCGATGTACCAGGTAAAGCCCTATC-3′) and reverse (5′-CTTAAGGAGCTTGAGGGCCGTGTTAAAAG-3′); GAPDH, forward (5′-GAAGGACTCATGACCACAG-3′) and reverse (5′-CTTCACCACCTTCTTGATG-3′). Products were analyzed by electrophoresis on 1% agarose gels.

Western blot analysis

After measuring the protein concentration of the lysates using a Bradford Protein Assay Kit (Bio-Rad, USA), equal amounts (25 μg) of protein were separated by 10-15% sodium dodecyl sulfate-polyacrylamide gel electrophoresis (SDS-PAGE) and transferred to nitrocellulose membranes. After membranes were blocked in Tris buffered saline-Tween (TBST) containing 5% skim milk for 1 h at room temperature, immunoblotting was performed by incubating overnight at 4°C with the corresponding primary antibody in 5% skim milk and then with secondary antibody conjugated to horseradish peroxidase (HRP) for 1 h. After washing, the band of interests was visualized using a model LAS-3000 luminescent image analyzer (Fujifilm, Japan).

Immunofluorescence assay

Cells were seeded in two-well chamber slides (Nalge Nunc, USA) at a density of 1×10^4 per well and infected with lentivirus containing sh-DX2 and sh-scr for 24 h. After 48 h incubation, slides were washed with phosphate buffered saline (PBS) and fixed in 4% paraformaldehyde for 10 min at 37°C. Cells were washed and fixed again with a 1:1 (v/v) mixture of methanol and acetone. After being blocked with 3% bovine serum albumin (BSA) in TBST for 1 h, cells were incubated in a 1:50 dilution of primary antibody overnight at 4°C, washed and incubated in a 1:500 dilution of FITC-conjugated secondary antibody for 2 h at room temperature. Nuclei were stained with DAPI for 30 min in the dark. After washing, coverslips were mounted using Dako Cytomation Faramount Aqueous Mounting Medium (Dako North America, USA), and the slides were visualized using a fluorescence microscope (Nikon, Japan).

Cy3-labeled glucose uptake

Cells were cultured on glass and infected with lentivirus containing sh-DX2 and sh-scr for 24 h. After an additional 48 h incubation, 12.5 μM of Cy3-labeled glucose (Park et al., 2007) was added and the live cells were monitored using confocal laser scanning microscopy (CLSM) within 15 min.

Luciferase assay

Cells were grown in six-well plates and infected with sh-DX2 and sh-scr. After 24 h incubation, cells were transfected with bicistronic reporter gene for 24 h. The next day, cells were washed twice in ice-cold PBS, extracted in passive lysis buffer (Promega, USA) and assayed for firefly and *Renilla* luciferase activities, according to the manufacturer's instructions. Firefly

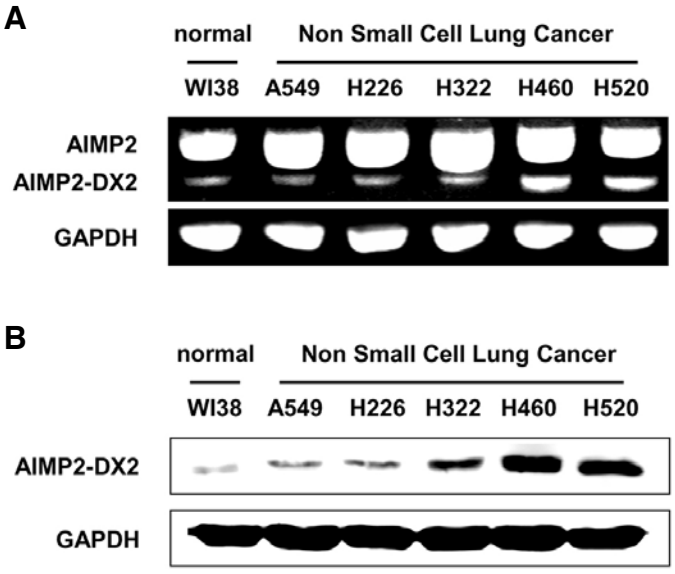

Fig. 1. Human AIMP2-DX2 expressions in lung cell lines. (A) Expressions of AIMP2-DX2 in lung cell lines were determined by RT-PCR. The upper bands showAIMP2 mRNA expression and the lower bands indicate expression of AIMP2-DX2 mRNA. (B) AIMP2-DX2 protein expression in several lung cell lines determined by Western blot analysis. Twenty-five micrograms of protein lysate from several lung cell lines were loaded into each well and the proteins resolved by 12% SDS-PAGE. Following transfer to a nitrocellulose membrane, Western blot was conducted using anti-AIMP2-DX2 and goat anti-mouse HRP-conjugated IgG as the primary and secondary antibody, respectively.

luciferase represents cap-dependent while *Renilla* luciferase activity represents cap-independent protein translation.

Statistical analysis

Data are expressed as mean ± SE. Student's *t*-test was used for comparison between the two groups. Comparison of several groups was done with one-way ANOVA. All statistical analyses were performed using GraphPad Software version 4.02 (USA). $^{*}p < 0.05$ was considered significant and $^{**}p < 0.01$ and $^{***}p < 0.001$ highly significant compared to corresponding control. Quantification of Western blot analysis was performed using Multi Gauge version 2.02 program (Fujifilm).

RESULTS

Expression of AIMP2-DX2 in human lung cell lines

Human AIMP2 mRNA consists of 963 base pairs. But, in several cancer cell lines, it also presents a smaller transcript (756 base pairs). Our RT-PCR data clearly confirmed such a pattern (Fig. 1A). The smaller transcript is the alternative splicing from of AIMP2 lacking exon 2 (AIMP2-DX2), which is specifically expressed in several lung cell lines. The expression levels of different lung cell lines were detected by RT-PCR and Western blot analysis. NCI-H460 and -H520 cell lines showed elevated expression of AIMP2-DX2 compared to other cell lines (Figs. 1A and 1B).

Structure and down-regulation of AIMP2-DX2 mRNA and protein expression in NCI-H460 cells

Figure 2A depicts the exon structure of AIMP2 and AIMP2-DX2. The siRNA primers were designed targeting the junction sequences between exons 1 and 3 of AIMP2. In the Figure, the underlined and italicized portions indicate exon 1 and exon 3 sequences of AIMP2, respectively. NCI-H460 cells were infected with lentivirus expressing either of two different shRNAs against AIMP2-DX2. As a shRNA control, NCI-H460 cells were infected with lentivirus delivered sh-scr. Both shRNA lentiviruses targeting AIMP2-DX2 decreased the mRNA levels as determined by RT-PCR analysis (Fig. 2B). Western blot data confirmed the RT-PCR results (Fig. 2C). sh-DX2 infected cells displayed a significant decrease in protein level of AIMP2-DX2. With 10 ng/ml of AIMP2-DX2, based on a concentration study (data not shown), cells were infected for 0, 12, 24 and 48 h. The level of AIMP2-DX2 was clearly decreased after 12 h (Fig. 2D). Expression of AIMP2-DX2 in the cytosol was further confirmed by an immunofluorescence assay. A reduction in fluorescence intensity was evident in sh-DX2 infected cells compared with control and sh-scr infected cells (Fig. 2E).

Down-regulation of AIMP2-DX2 reduce the rate of glucose uptake in NCI-H460 cells

To examine the uptake of glucose in sh-DX2 infected cells, 12.5 μM of Cy3-labeled glucose was used for live cell imaging (Park et al., 2007). The uptake of Cy3-labeled glucose by NCI-H460 cells reached the maximum after 15 min. No differences in Cy3-labeled glucose uptake were detected between control cells and sh-scr infected cells. However, significantly reduced Cy3-labeled glucose uptake was detected in sh-DX2 infected cells compared with control or sh-scr infected cells by CLSM (Fig. 3A). Statistically significant correlations were detected between sh-DX2 infected cells and both control and sh-scr infected cells. Statistical difference of Cy3-labeled glucose uptake in the cytosol was observed after 6 min (Fig. 3B).

Down-regulation of AIMP2-DX2 decreases the expression of glucose transporter proteins

The uptake of Cy3-labeled glucose is inhibited by D-glucose but not by L-glucose, and Cy3-labeled glucose is taken up through a glucose specific transporter system, not by passive diffusion *in vitro* (Park et al., 2007). Glucose uptake in NSCLC is relative to glucose transporter type I (Glut-1) expression (Younes et al., 1996). Presently, protein levels of Glut-2, Glut-4 and Glut-1 were decreased by lentiviral sh-DX2 infection. Glut-3 expression did not show such pattern as detected by Western blot analysis (Fig. 4A). Immunofluorescence analysis of Glut-1, Glut-2 and Glut-4 expression in NCI-H460 cells clearly confirmed the results of Western blot analysis (Fig. 4B).

Name	Target sequence (5'→3')	Size (bp)	Nucleotide position
si-AIMP2-DX2 #4	GCTGGCCACGTGCAGGA*TTAC*	21	121~141
si-AIMP2-DX2 #5	CACGTGCAGGA*TTACGGGGC*	20	127~146

* Underline : Exon1 seq. * *Italic* : Exon3 seq.

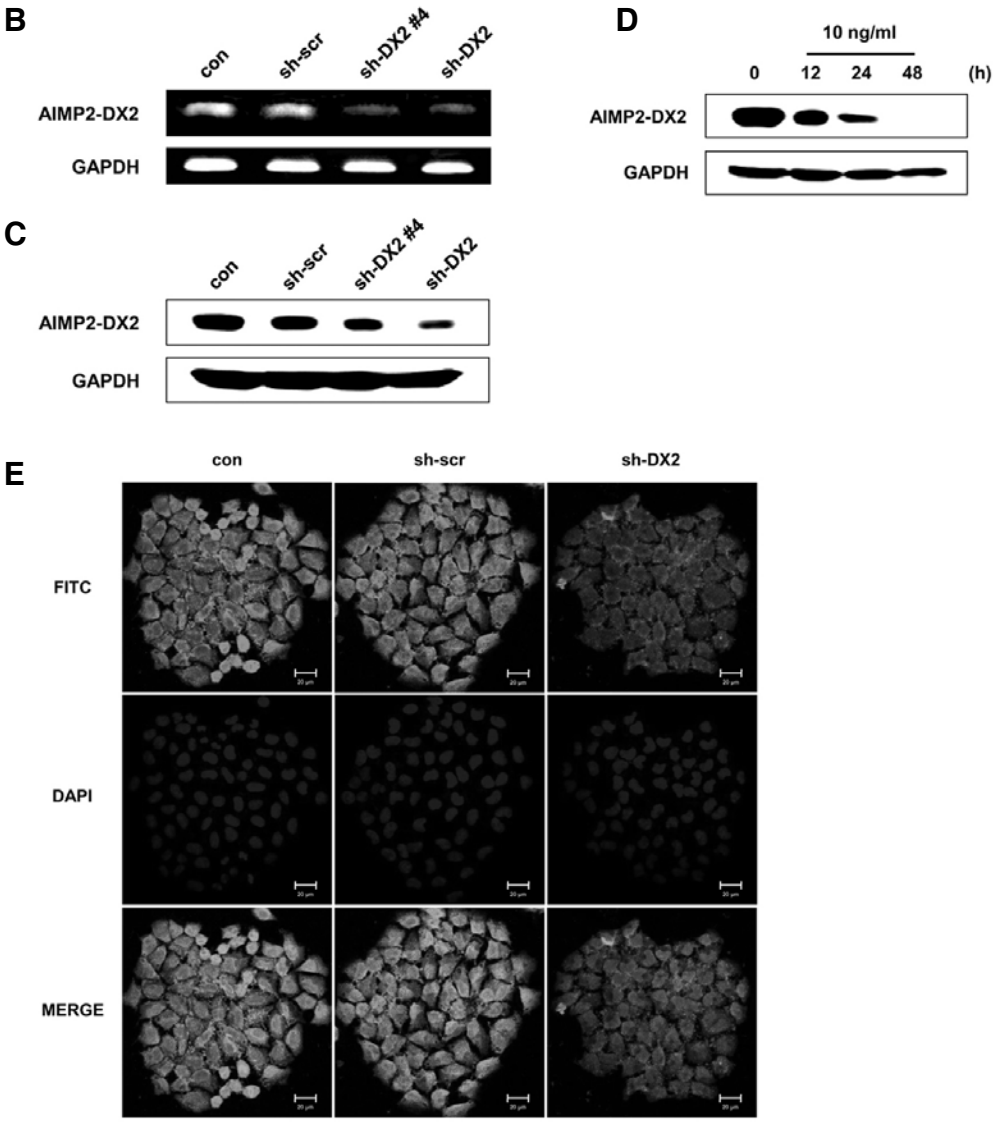

Fig. 2. Down-regulation of AIMP2-DX2 mRNA and protein expres-sion in NCI-H460 cells. (A) Structural schema of AIMP2 and AIMP2-DX2 gene. Underlines and italics ind-icate exon 1 and exon 3 sequence of AIMP2, respectively. (B) RT-PCR and (C) Western blot analysis of AIMP2-DX2. Cells were infected with lentiviral vector-mediated shRNA targeting sh-DX2 #4, sh-DX2 and sh-scr as a control for 24 h. After an additional incubation for 48 h, cells were harvested for the aforementioned analyses. (D) AIMP2-DX2 expression in various time points after infection. (E) Localization of AIMP2-DX2 in NCI-H460 cells were detected by immunofluore-scence assay using fluorescence microscopy. Infected cells with either sh-DX2 or sh-scr were fixed and incubated with primary antibody, anti-AIMP2-DX2, followed by fluorescent secondary antibody, goat anti-mouse FITC-conjugated IgG. Top, localization of anti-AIMP2-DX2 (green *via* FITC); Middle, nucleus (blue ia DAPI staining); and Bottom, merged signals. The scale bar represents 20 μm.

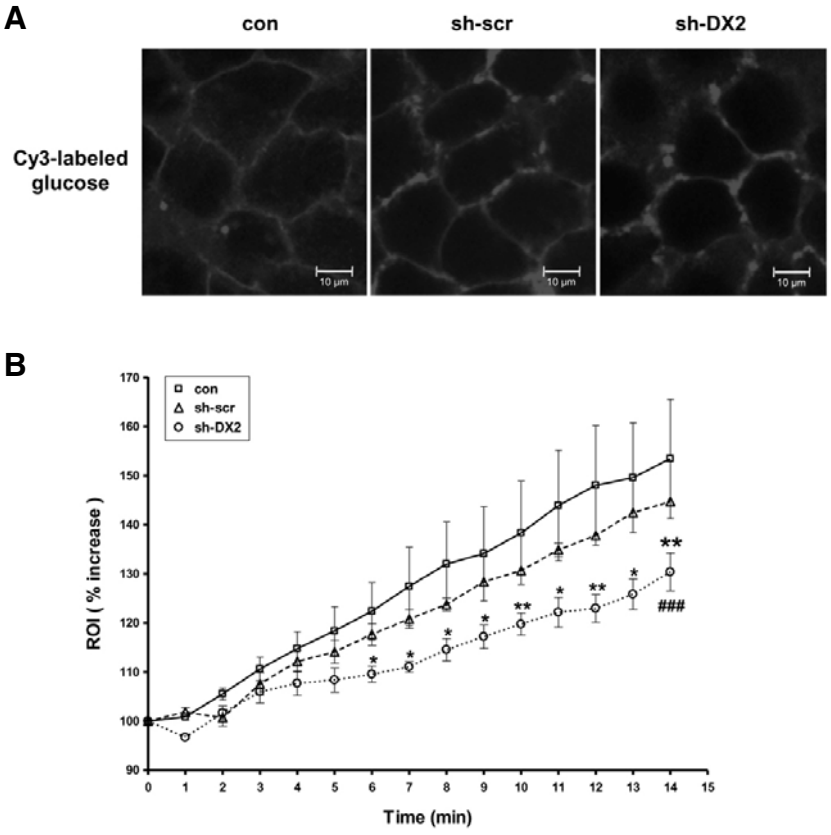

Fig. 3. Effect of sh-DX2 on Cy3-labeled glucose uptake in NCI-H460 cells. (A) Fluorescence images in NCI-H460 cells were moni-tored by live-cell imaging with CLSM. Infected cells were treated with 12.5 μM of Cy3-labled glucose. The scale bar represents 10 μm. (B) Fluorescence intensities were determined by continuous measurement of regions of interest (ROI) of three independent cells. Open square, control; open triangle, sh-scr; and open circle, sh-DX2. $^{*}p < 0.05$, $^{**}p < 0.01$, $^{***}p < 0.001$ significantly increased compared to sh-scr, and $^{###}p < 0.001$ significantly increased compared to control.

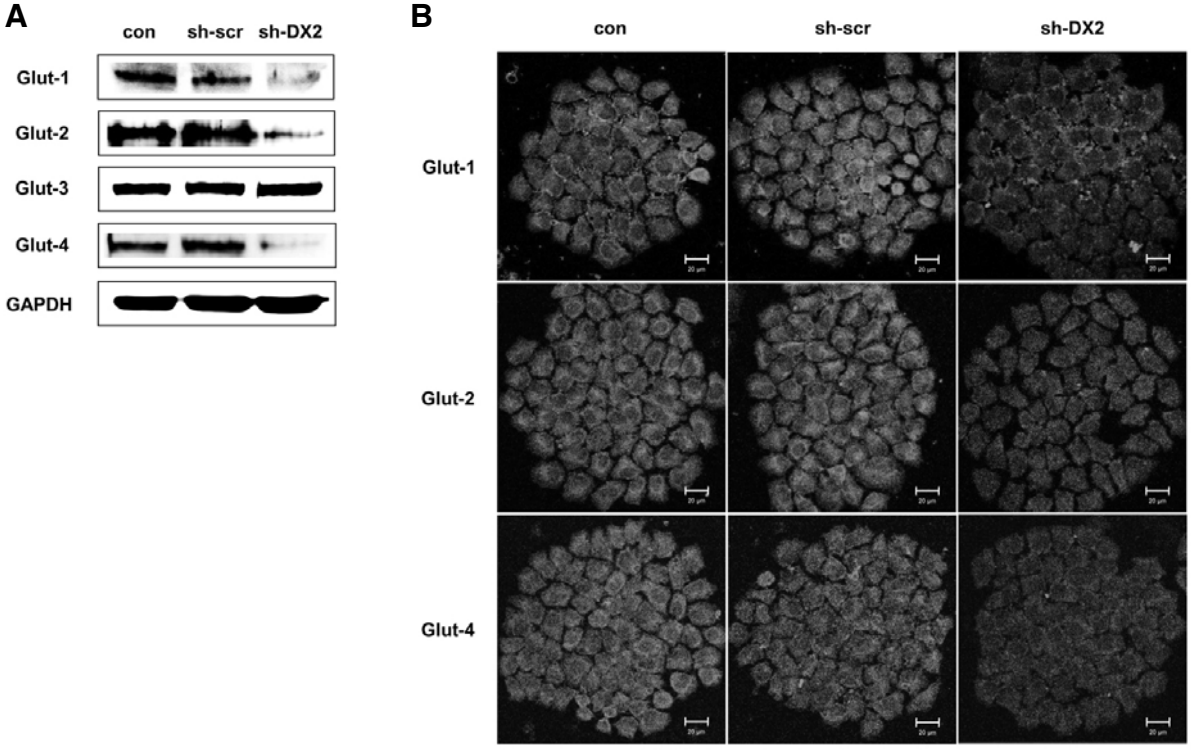

Fig. 4. Effects of sh-DX2 on glucose transporters (Gluts). The ex-pression of glucose transporter (Glut) proteins in infected cells was detected by Western blot analysis (A) and an immunofluorescence assay using fluorescence microscopy (B). sh-DX2 and sh-scr infected cells were fixed, washed and incubated with primary antibodies (anti-Glut-1, anti-Glut-2, and anti-Glut-4) followed by fluorescent secondary antibody, goat anti-rabbit FITC-conjugated IgG. The scale bar represents 20 μm.

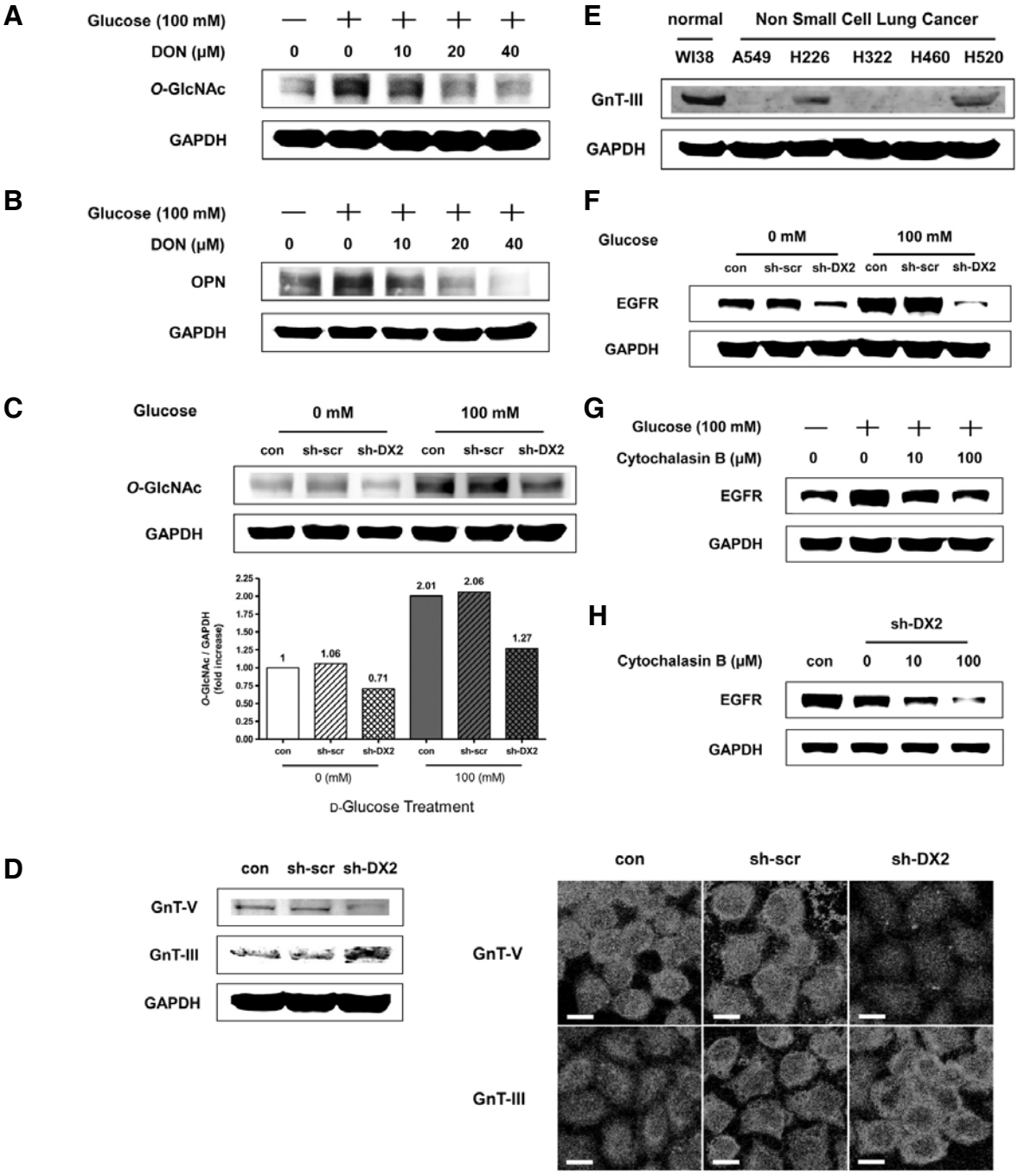

Fig. 5. Overexpression of EGFR protein by high glucose *via* glycosyltransferase (GnT). (A) Effect of DON on glucose-induced *O*-GlcNAc. Cells were pre-treated with DON (10, 20 and 40 μM), GFAT inhibitor for 30 min, then 100 mM of glucose was added for additional 2 h. and then harvested for Western blot analysis. (B) Expression of *O*-GlcNAc protein was detected by Western blot (Upper panel). Densitometric analysis of the bands corresponding to *O*-GlcNAc (Lower panel). Cells were infected with lentivirus containing sh-DX2 and sh-scr for 24 h. After additional incubation for 48 h, cells were treated with 100 mM of glucose for 2 h. (C) The expression of glycosyltransferases (GnTs) in infected cells were detected by Western blot analysis (Upper panel) and immunofluorescence assay using fluorescence microscope (Lower panel). sh-DX2 and sh-scr infected cells were fixed, washed, and incubated with primary antibodies, anti-GnT-V, and anti-GnT-III, followed by fluorescent secondary antibody. The scale bar represents 10 μm. (D) GnT-III protein expression in several lung cell lines was determined by Western blot analysis. Twenty-five micrograms of protein lysate from several lung cell lines loaded into each well and the proteins were separated by 12% SDS-PAGE. Following transfer of the proteins to a nitrocellulose membrane, the membrane was incubated with anti-GnT-III and rabbit anti-goat HRP-conjugated IgG as the primary and secondary antibody, respectively. (E) Expression of EGFR protein was detected by Western blot. Cells were infected with lentivirus containing sh-DX2 and sh-scr for 24 h. After additional incubation for 48 h, cells were treated with 100 mM of glucose for 2 h and then harvested for Western blot analysis. (F) Effect of cytochalasin B on glucose-induced EGFR. Cells were pre-treated with the glucose transport inhibitor cytochalasin B (10 or 100 μM) for 10 min, then 100 mM of glucose was added for an additional 2 h. EGFR and GAPDH were detected by Western blot analysis. (G) Effect of cytochalasin B on EGFR protein level in sh-DX2 treated cells. Cells were infected with lentivirus containing sh-DX2 for 24 h, and treated with cytochalasin B (10 or 100 μM) for 48 h. The cells were lysed and 25 μg of protein was used for Western blot analysis.

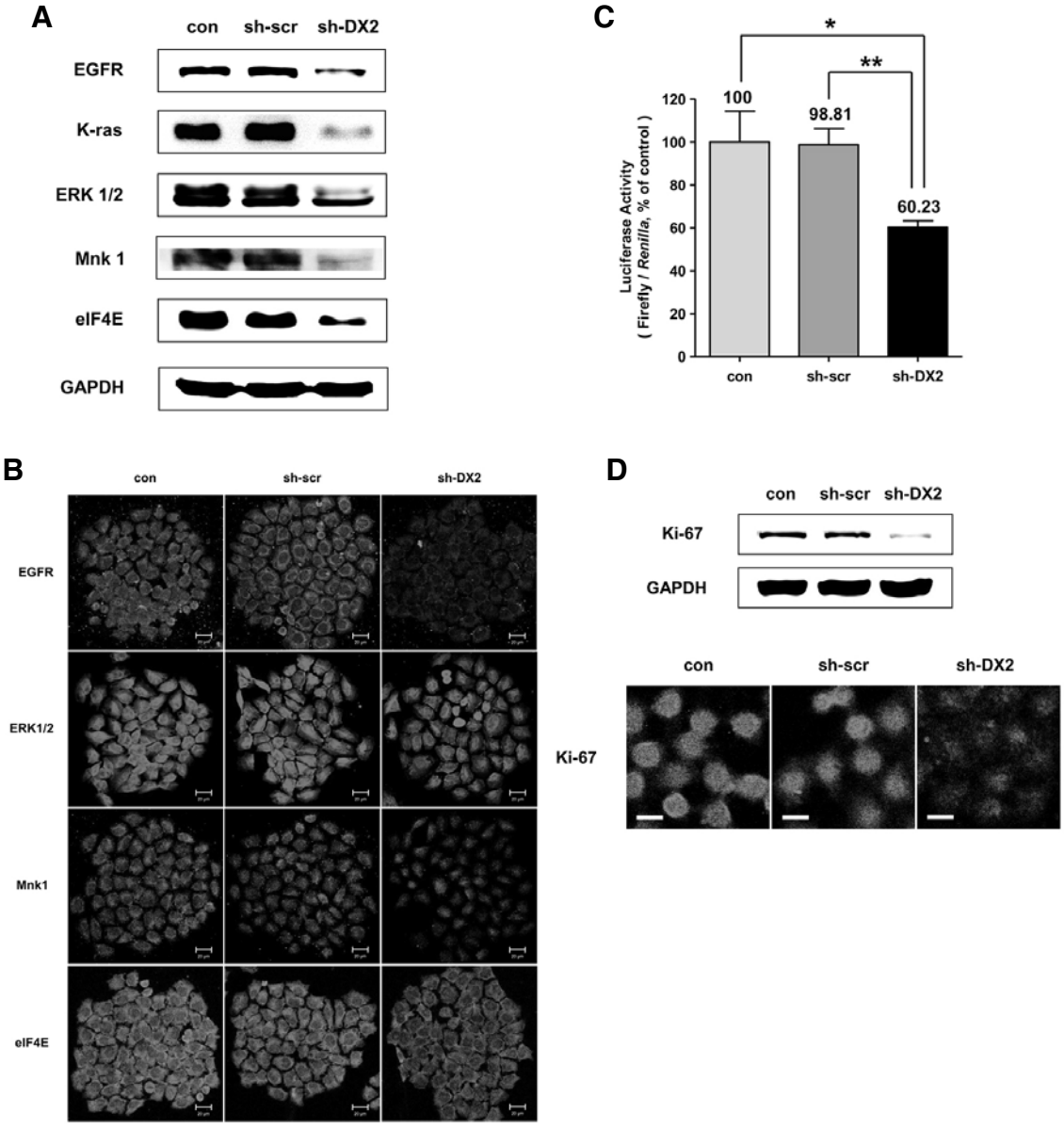

Fig. 6. Effects of sh-DX2 on EGFR/MAPK signal and cell prolix-feration. Reduced expression of EGFR/MAPK signal pathway relative proteins by sh-DX2 infection. (A) Cells were infected with lentivirus containing sh-DX2 and sh-scr for 24 h and sequentially incubated with fresh medium for 48 h. After 48 h incubation, cells were lysed and 25 μg was used for Western blot analysis. (B) Fluorescence imaging of the EGFR/MAPK relative proteins. Infected cells with lentivirus containing sh-DX2 and sh-scr were fixed and assayed using immunostaining for EGFR, ERK1/2, Mnk1 and eIF4E. The scale bar represents 20 μm. (C) For dual luciferase assay, cells were transfected with bicistronic reporter construct, pcDNA-fLUC-polIRES-rLUC, for 24 h following infection with sh-DX2 and sh-scr. The next day, cells were lysed and assayed for firefly and *Renilla* luciferase activities. Values are the mean ± SE of three independent experiments. *$p < 0.05$ vs control, **$p < 0.01$ vs sh-scr. (D) The expression of Ki-67 in infected cells was detected by Western blot analysis (Upper panel) and immunofluorescence assay using fluorescence microscope (Lower panel). The scale bar represents 10 μm.

High glucose induced EGFR expression *via* glycosyltransferase (GnT) in the Golgi apparatus

To investigate whether glucose could induce the hexosamine pathway, cells were treated with various concentrations of glutamine fructose-6-phosphate amidotransferase (GFAT) inhibitor (DON) in the presence of glucose and the expression levels of *O*-GlcNAc were analyzed by Western blot. The *O*-GlcNAc protein levels were decreased in a dose-dependent manner (Fig. 5A). OPN as a highly phosphorylated and glycosylated protein with five *O*-glycosylation sites was employed to detect the changes in *O*-glycosylation. Increased OPN protein level was evident in the presence of high glucose. The dose-dependent decrease of OPN expression was observed in the presence of different concentrations of DON (Fig. 5B). Because the protein levels of *O*-GlcNAc were also detected in infected cells in the presence and absence of glucose, the results indicated that high glucose (100 mM) markedly increased the protein levels of *O*-GlcNAc in control and sh-scr infected cells.

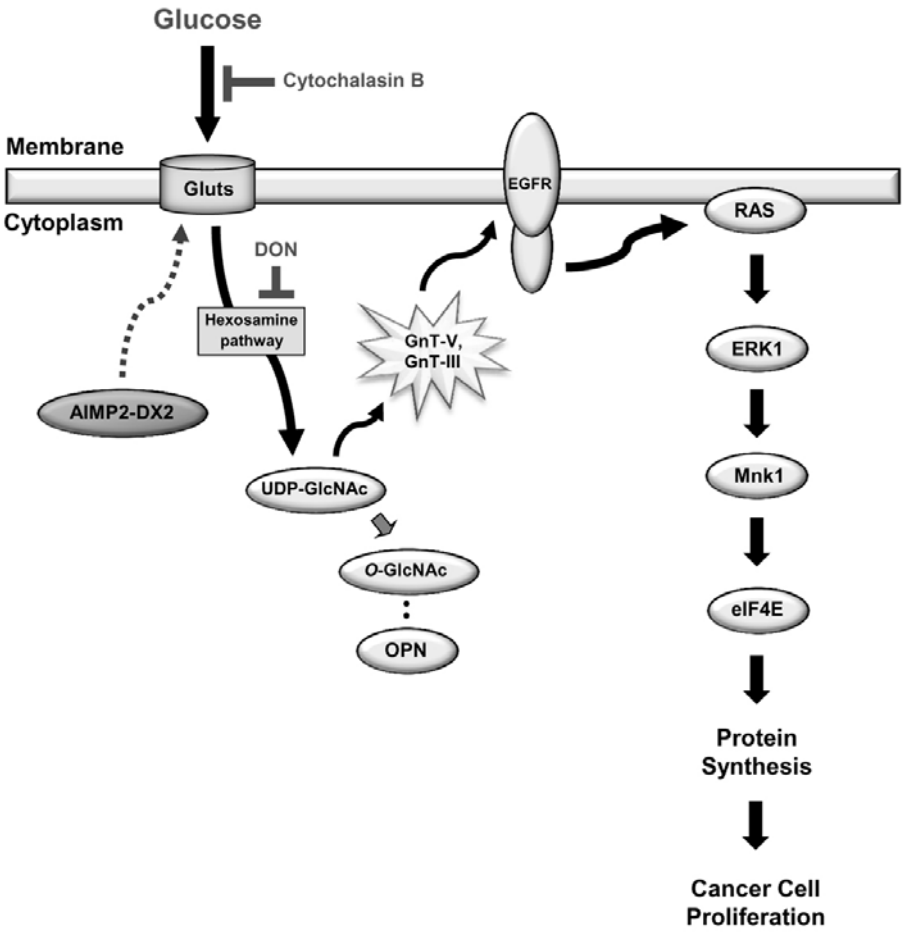

Fig. 7. Schematic signal pathway by siRNA targeting AIMP2-DX2 in NCI-H460 cells. Based on our studies, AIMP2-DX2 has an effect on Gluts expression. When Glut expression decreases due to AIMP2-DX2 down-regulation, glucose influx decreases and this decreased signal is transmited to EGFR via glycosyltransferases, affecting the EGFR/MAPK pathway. The delivered signal, as a whole, causes a decrease of eIF4E expression, which may lead to transcription reduction resulting decreased cell proliferation. Wang et al. (2009) and Guo et al. (2007) showed the link between GnT-V/GnT-III and EGFR.

However, sh-DX2 infected cells did not show the same pattern. Densitometric analysis clearly confirmed the Western blot results (Fig. 5C). The effects of sh-DX2 on glycosyltransferases in the Golgi apparatus were investigated. sh-DX2 infected cells decreased the protein level of GnT-V whereas an increase in protein level of GnT-III was observed by Western blot. The findings were further supported by immunofluorescence analysis of GnT-V and GnT-III (Fig. 5D). Furthermore, we determined the expression levels of GnT-III in different lung cell lines by Western blot. Normal cell line (WI-38) showed high expression level of GnT-III, whereas low expression levels in lung cancer cell lines were observed. Among the lung cancer cell lines, NCI-H226 and NCI-H520 showed higher expression compared to other examined lung cancer cell lines (Fig. 5E). High glucose induced an increase in EGFR protein expression of control cells and sh-scr infected cells, whereas sh-DX2 infected cells did not show such pattern of change. These results suggest that up-regulation of EGFR in high glucose conditions takes place through an AIMP2-DX2-dependent mechanism (Fig. 5F). To study the effect of high glucose on EGFR, the glucose transport inhibitor, cytochalasin B, was used. Pretreatment with the inhibitor suppressed glucose-induced EGFR expression (Fig. 5G). In sh-DX2 infected cells, cytochalasin B affected the EGFR protein expression in a dose-dependent manner (Fig. 5H).

Down-regulation of AIMP2-DX2 suppresses EGFR/MAPK signals and cell proliferation

To determine whether EGFR/MAPK signaling molecules were affected by sh-DX2 infection, Western blot and immunofluorescence analysis were carried out in infected cells. Western blot analysis using specific antibodies to various MAPKs revealed that the response of NCI-H460 cells to sh-DX2 was selective and specific because decreases of EGFR, K-ras, ERK1/2, Mnk1 and eIF4E expressions were clearly observed (Fig. 6A). Immunofluorescence analysis of EGFR, ERK1/2, Mnk1 and eIF4E apparently confirmed such pattern (Fig. 6B). Furthermore, dual luciferase activities were measured to study the changes in protein translation of infected cells. The relative ratio of firefly/*Renilla* (Cap-dependent/Cap-independent) activities was markedly decreased in sh-DX2 infected cells compared with control (p = 0.034) and sh-scr (p = 0.003) infected cells, indicating that the infection of cells with sh-DX2 reduced cap-dependent protein translation (Fig. 6C). In addition, the effect of sh-DX2 on cell proliferation was investigated. sh-DX2 infected cells clearly had decreased quantity of Ki-67 (cell proliferation marker) protein as detected by Western blot. Immunofluorescence analysis distinctively re-confirmed that sh-DX2 decreased the expression level of Ki-67 (Fig. 6D).

DISCUSSION

AIMP2-DX2 counteracts with AIMP2 and overexpresses in human lung cancer

AIMP2 is a novel tumor suppressor, which has a unique role in TGF-β signaling via interaction with Smad 2/3 Kim (2004, 2005). The observation that the level of AIMP2 is markedly reduced, regardless of TGF-β, is evidence that the generation of AIMP2-DX2 leads to loss of AIMP2 activity. AIMP2-DX2 is closely associated with tumorigenesis by its mediated induction of the decrease of AIMP2 level. Suppression of AIMP2-DX2 expression may thus provide important therapeutic applications. Presently, down-regulation of AIMP2-DX2 expression using lentiviral vector-mediated shRNA was demonstrated in lung cancer cells.

Effects of AIMP2-DX2 on glucose uptake and transporters

The high metabolism and increased rates of glucose consumption of cancer cells are associated with changes in the levels and isoenzyme compositions of glycolytic enzymes (Golshani, 1992) and the overexpression of Gluts (Brown and Wahl, 1993; Merrall et al., 1993; Yamamoto et al., 1990) compared with the surrounding normal tissues. Changes in the rate of glucose uptake and overexpression of glucose transporters are also associated with adaption to hypoxia partly due to increased dependency on glycolysis as an energy source (Ismail-Beigi, 1993; Merrall et al., 1993), a condition that may arise in rapidly growing tumors (Vaupel et al., 1989). These changes in glucose metabolism have been successfully used to diagnose of stage and monitor tumor response to therapy by (2-[fluorine-18]-fluoro-2-deoxy-D-glucose (FDG) positron emission tomography imaging (Abdel-Dayem et al., 1994). The FDG analogue, 2-[*N*-(7-nitrobenz-2-oxa-1,3-diazol-4-yl)-amino]-2-deoxy-D-glucose (2-NBDG), has been also widely applied in various studies for tumor imaging and the examination of Glut-related cell metabolism (Lloyd et al., 1999; Natarajan and Srienc, 2000; Oh et al., 2002; Yamada et al., 2000; Yoshioka et al., 1996). However, 2-NBDG is applicable only in a non-physiological sugar-depleted environment. In this study, we used a novel fluorescence-labeled glucose analogue, Cy3-linked *O*-1-glycosylated glucose, which can behave as D-glucose. Cy3-labeled glucose is tolerant to intense light sources and can be applied in a bioassay system without glucose starvation (Park et al., 2007). Our results showed that the down-regulation of AIMP2-DX2 significantly decreased glucose uptake, which may lead to reduction of glucose consumption rate in sh-DX2 treated cells.

Glucose uptake in NSCLC is related to Glut-1 expression, which is a significant indicator of poor prognosis (Minami et al., 2002; Younes et al., 1997). Glut-1 expression indicates increased glucose uptake as well as increased energy consumption (Younes et al., 1996). Kalsi et al. (2008) reported the expression of Glut-2 and Glut-4 in the human lung adenocarcinoma epithelial cell line. These proteins are also overexpressed in various tumor cells (Godoy et al., 2006). Presently, sh-DX2 decreased Glut-1, Glut-2 and Glut-4 expression in lung cancer cells. These results indicate profound changes in energy metabolism that play an important role in cancer progression.

Effects of AIMP2-DX2 on glycosyltransperase in the Golgi apparatus and EGFR expression

GnT-V, GlcNAc-β1-6, plays a pivotal role in the processing of N-linked glycoproteins and influences cancer progression and metastasis. Gene expression of GnT-V is regulated by a transcriptional factor involved in angiogenesis and invasion of tumor cells (Taniguchi et al., 1999). When the formation of the product of GnT-V is inhibited by overexpression of GnT-III, lung metastasis of melanoma cells is suppressed (Yoshimura et al., 1995). GnT-III catalyzes the addition of bisecting GlcNAc (β-1,4-GlcNAc branching) to biantennary sugar chains and prevents the subsequent actions of GnT-V and GnT-IV (Sasai et al., 2002; Sultan et al., 1997; Wang et al., 1997). GnT-III is an antagonist of GnT-V in terms of diminished metastatic potential and integrin-mediated cell migration (Chakraborty and Pawelek, 2007; Zhao et al., 2006). Presently, it was clear that sh-DX2 decreased GnT-V and increased GnT-III expression, which may alter N-linked glycosylation leading to regulation of N-glycoproteins. Interestingly, we also demonstrated overexpression of GnT-III in a normal lung cell line (WI-38) and squamous cell lines (NCI-H226 and NCI-H520) suggesting low metastatic activity of squamous carcinoma compared to large-cell carcinoma and adenocarcinoma.

Effects of AIMP2-DX2 on EGFR/MAPK signaling pathway

High glucose transactivates EGFR, independent of local up-regulation of EGF protein, potentially amplifying the functional response (Saad et al., 2005). MAPK has been implicated in long-term cellular effects such as gene transcription and cell proliferation and differentiation (Srinivasa et al., 2012; Sugden and Clerk, 1997). MAPK activation is EGFR-dependent in most cells. It has also been reported that activated EGFR can stimulate the MAPK signaling pathway (Kanno et al., 2003). Our findings showed the suppressive effect of sh-DX2 on EGFR expression in the presence of different glucose concentrations. Inhibition by the known glucose transport inhibitor cytochalasin B suggests that sh-DX2 may suppress cell proliferation by inhibiting EGFR expression. Our results clearly showed that expression of K-ras, ERK1/2, Mnk1 and eIF4E, which are involved in the EGFR/MAPK signaling pathway, were generally decreased by sh-DX2. Decreased eIF4E as an important protein of the translation initiation complex resulted in a decrease of cap-dependent protein translation that may play a key role in cell proliferation and growth. Ki-67 is a marker for cell proliferation of solid tumors (Steck and el-Naggar, 1994) and is overexpressed in clinical stage IA lung adenocarcinomas (Watanabe et al., 2006). Presently, lentiviral delivery of sh-DX2 decreased Ki-67 expression, which may inhibit cancer cell proliferation.

In conclusion, our results clearly demonstrate that lentiviral vector-mediated siRNA down-regulation of AIMP2-DX2 can inhibit glucose uptake and suppress the EGFR/MAPK signaling pathway. As a result, decreased protein synthesis by sh-DX2 may regulate cancer cell growth. These results suggest that AIMP2-DX2 may be a relevant therapeutic target for lung cancer, and that the sh-DX2 lentiviral delivery system can be an appropriate method for lung cancer therapy.

ACKNOWLEDGMENTS

This work was supported by the National Research Foundation grants (NRF-2012-0001116) from the Ministry of Education, Science and Technology (MEST) and M.H. Cho was also partially supported by the Research Institute for Veterinary Science, Seoul National University.

REFERENCES

Abdel-Dayem, H.M., Scott, A., Macapinlac, H., and Larson, S. (1994). Tracer imaging in lung cancer. Eur. J. Nucl. Med. *21*, 57-81.

Brown, R.S., and Wahl, R.L. (1993). Overexpression of Glut-1 glucose transporter in human breast cancer. An immunohistochemical study. Cancer *72*, 2979-2985.

Chakraborty, A.K., and Pawelek, J. (2007). Beta1,6-branched oligosaccharides regulate melanin content and motility in macro-

phage-melanoma fusion hybrids. Melanoma Res. *17*, 9-16.
Duncan, R., Bazar, L., Michelotti, G., Tomonaga, T., Krutzsch, H., Avigan, M., and Levens, D. (1994). A sequence-specific, single-strand binding protein activates the far upstream element of c-myc and defines a new DNA-binding motif. Genes Dev. *8*, 465-480.
Godoy, A., Ulloa, V., Rodriguez, F., Reinicke, K., Yañez, A.J., García, M.L., Medina, R.A., Carrasco, M., Barberis, S., Castro, T., et al. (2006). Differential subcellular distribution of glucose transporters GLUT1-6 and GLUT9 in human cancer: ultrastructural localization of GLUT1 and GLUT5 in breast tumor tissues. J. Cell Physiol. *207*, 614-627.
Golshani, S. (1992). Insulin, growth factors, and cancer cell energy metabolism: an hypothesis on oncogene action. Biochem. Med. Metab. Biol. *47*, 108-115.
Guo, H.B., Randolph, M., and Pierce, M. (2007). Inhibition of a specific N-glycosylation activity results in attenuation of breast carcinoma cell invasiveness-related phenotypes: inhibition of epidermal growth factor-induced dephosphorylation of focal adhesion kinase. J. Biol. Chem. *282*, 22150-22162.
Ismail-Beigi, F. (1993). Metabolic regulation of glucose transport. J. Membr. Biol. *135*, 1-10.
Kalsi, K.K., Baker, E.H., Medina, R.A., Rice, S., Wood, D.M., Ratoff, J.C., Philips, B.J., and Baines, D.L. (2008). Apical and basolateral localisation of GLUT2 transporters in human lung epithelial cells. Pflugers Arch. *456*, 991-1003.
Kanno, H., Horikawa, Y., Hodges, R.R., Zoukhri, D., Shatos, M.A., Rios, J.D., and Dartt, D.A. (2003). Cholinergic agonists transactivate EGFR and stimulate MAPK to induce goblet cell secretion. Am. J. Physiol. Cell Physiol. *284*, 988-998.
Kim, M.J., Park, B.J., Kang, Y.S., Kim, H.J., Park, J.H., Kang, J.W., Lee, S.W., Han, J.M., Lee, H.W., and Kim, S. (2003). Downregulation of FUSE-binding protein and c-myc by tRNA synthetase cofactor p38 is required for lung cell differentiation. Nat. Genet. *34*, 330-336.
Kim, S. (2004, 2005). Aimp2-dx2 and its uses. Korean Pat. Appln. (2004, 2005). 10-2004-0097164, 10-2005-39073.
Ko, H.S., von Coelln, R., Sriram, S.R., Kim, S.W., Chung, K.K., Pletnikova, O., Troncoso, J., Johnson, B., Saffary, R., Goh, E.L., et al. (2005). Accumulation of the authentic parkin substrate aminoacyl-tRNA synthetase cofactor, p38/JTV-1, leads to catecholaminergic cell death. J. Neurosci. *25*, 7968-7978.
Lau, K.S., Partridge, E.A., Grigorian, A., Silvescu, C.I., Reinhold, V.N., Demetriou, M., and Dennis, J.W. (2007). Complex N-glycan number and degree of branching cooperate to regulate cell proliferation and differentiation. Cell *129*, 123-134.
Lloyd, P.G., Hardin, C.D., and Sturek, M. (1999). Examining glucose transport in single vascular smooth muscle cells with a fluorescent glucose analog. Physiol. Res. *48*, 401-410.
Merrall, N.W., Plevin, R., and Gould, G.W. (1993) Growth factors, mitogens, oncogenes and the regulation of glucose transport. Cell Signal. *5*, 667-675.
Minami, K., Saito, Y., Imamura, H., and Okamura, A. (2002). Prognostic significance of p53, Ki-67, VEGF and Glut-1 in resected stage I adenocarcinoma of the lung. Lung Cancer *38*, 51-57.
Natarajan, A., and Srienc, F. (2000). Glucose uptake rates of single *E. coli* cells grown in glucose-limited chemostat cultures. J. Microbiol. Methods *42*, 87-96.
Oh, K.B., and Matsuoka, H. (2002). Rapid viability assessment of yeast cells using vital staining with 2-NBDG, a fluorescent derivative of glucose. Int. J. Food Microbiol. *76*, 47-53.
Park, S.G., Ewalt, K.L., and Kim, S. (2005). Functional expansion of aminoacyl-tRNA synthetases and their interacting factors: new perspectives on housekeepers. Trends Biochem. Sci. *30*, 569-574.
Park, J., Lee, H.Y., Cho, M.H., and Park, S.B. (2007). Development of a cy3-labeled glucose bioprobe and its application in bioimaging and screening for anticancer agents. Angew. Chem. Int. Ed. Engl. *46*, 2018-2022.
Saad, S., Stevens, V.A., Wassef, L., Poronnik, P., Kelly, D.J., Gilbert, R.E., and Pollock, C.A. (2005). High glucose transactivates the EGF receptor and up-regulates serum glucocorticoid kinase in the proximal tubule. Kidney Int. *68*, 985-997.
Sasai, K., Ikeda, Y., Fujii, T., Tsuda, T., and Taniguchi, N. (2002). UDP-GlcNAc concentration is an important factor in the biosynthesis of β1,6-branched ligosaccharides: regulation based on the kinetic properties of *N*-acetylglucosaminyltransferase V. Glycobiology *12*, 119-127.
Srinivasa, K., Kim, J., Yee, S., Kim, W., and Choi, W. (2012). A MAP kinase pathway is implicated in the pseudohyphal induction by hydrogen peroxide in Candica albicans. Mol. Cells *33*, 183-193.
Steck, K., and el-Naggar, A.K. (1994). Comparative flow cytometric analysis of Ki-67 and proliferating cell nuclear antigen (PCNA) in solid neoplasms. Cytometry *17*, 258-265.
Sugden, P.H., and Clerk, A. (1997). Regulation of the ERK subgroup of MAP kinase cascades through G protein-coupled receptors. Cell Signal. *9*, 337-351.
Sultan, A.S., Miyoshi, E., Ihara, Y., Nishikawa, A., Tsukada, Y., and Taniguchi, N. (1997). Bisecting GlcNAc structures act as negative sorting signals for cell surface glycoproteins in forskolin-treated rat hepatoma cells. J. Biol. Chem. *272*, 2866-2872.
Taniguchi, N., Miyoshi, E., Ko, J.H., Ikeda, Y., and Ihara, Y. (1999). Implication of N-acetylglucosaminyltransferases III and V in cancer: gene regulation and signaling mechanism. Biochim. Biophys. Acta *1455*, 287-300.
Vaupel, P., Kallinowski, F., and Okunieff, P. (1989). Blood flow, oxygen and nutrient supply, and metabolic microenvironment of human tumors: a review. Cancer Res. *49*, 6449-6465.
Wang, Q., Zhou, D., Shao, D., Shen, Z., and Gu, J. (1997). Effects of epidermal growth factor and insulin on the activity of N-acetylglucosaminyltransferase V. Biochem J. *324*, 543-545.
Wang, C., Yang, Y., Yang, Z., Liu, M., Li, Z., Sun, L., Mei, C., Chen, H., Chen, L., Wang, L., et al. (2009). EGF-mediated migration signaling activated by N-acetylglucosaminyltransferase-V via receptor protein tyrosine phosphatase kappa. Arch. Biochem. Biophys. *486*, 64-72.
Watanabe, K., Nomori, H., Ohtsuka, T., Naruke, T., Ebihara, A., Orikasa, H., Yamazaki, K., Uno, K., Kobayashi, T., and Goya, T. (2006). [F-18] Fluorodeoxyglucose positron emission tomography can predict pathological tumor stage and proliferative activity determined by Ki-67 in clinical stage IA lung adenocarcinomas. Jpn. J. Clin. Oncol. *36*, 403-409.
Yamada, K., Nakata, M., Horimoto, N., Saito, M., Matsuoka, H., and Inagaki, N. (2000). Measurement of glucose uptake and intracellular calcium concentration in single, living pancreatic beta-cells. J. Biol. Chem. *275*, 22278-22283.
Yamamoto, T., Seino, Y., Fukumoto, H., Koh, G., Yano, H., Inagaki, N., Yamada, Y., Inoue, K., Manabe, T., and Imura, H. (1990). Over- expression of facilitative glucose transporter genes in human cancer. Biochem. Biophys. Res. Commun. *170*, 223-230.
Yoshimura, M., Nishikawa, A., Ihara, Y., Taniguchi, S., and Taniguchi, N. (1995). Suppression of lung metastasis of B16 mouse melanoma by N-acetylglucosaminyltransferase III gene transfection. Proc. Natl. Acad. Sci. USA *92*, 8754-8758.
Yoshioka, K., Saito, M., Oh, K.B., Nemoto, Y., Matsuoka, H., Natsume, M., and Abe, H. (1996). Intracellular fate of 2-NBDG, a fluorescent probe for glucose uptake activity, in Escherichia coli cells. Biosci. Biotechnol. Biochem. *60*, 1899-1901.
Younes, M., Lechago, L.V., Somoano, J.R., Mosharaf, M., and Lechago, J. (1996). Wide expression of the human erythrocyte glucose transporter Glut1 in human cancers. Cancer Res. *56*, 1164-1167.
Younes, M., Brown, R.W., Stephenson, M., Gondo, M., and Cagle, P.T. (1997). Overexpression of Glut1 and Glut3 in stage I nonsmall cell lung carcinoma is associated with poor survival. Cancer *80*, 1046-1051.
Zhao, Y., Nakagawa, T., Itoh, S., Inamori, K., Isaji, T., Kariya, Y., Kondo, A., Miyoshi, E., Miyazaki, K., Kawasaki, N., et al. (2006). N-acetylglucosaminyltransferase III antagonizes the effect of N-acetylglucosaminyltransferase V on alpha3beta1 integrin-mediated cell migration. J. Biol. Chem. *281*, 32122-32130.